General Formulas for the Beam Properties of 1-D Bidirectional Leaky-Wave Antennas

Walter Fuscaldo, *Member, IEEE,* David R. Jackson, *Fellow, IEEE,* and Alessandro Galli, *Member, IEEE.*

***Abstract*—In this work we analyze the beam properties of *bidirectional* one-dimensional leaky-wave antennas (1-D LWAs). Specifically, it is found that, even in the *infinite-aperture* case, the beam properties considerably change for certain combinations of the phase and the attenuation constants, and different radiation regimes are identified here. New analytic formulas are provided to exactly evaluate the beamwidth of an infinite 1-D bidirectional LWAs operating in any radiating regime. However, when the *antenna truncation* is accounted for, the boundaries between the radiating regimes change as the radiation efficiency changes. Analytic formulas are therefore provided to accurately calculate such boundaries for any practical radiation efficiency. The interesting case of a finite-length bidirectional 1-D LWA radiating at *broadside* is then extensively discussed. With respect to previous beamwidth formulas found in the literature, the new formulas take into account the finiteness of the aperture, thus providing more useful and reliable results, especially in cases when the aperture truncation considerably affects the radiation efficiency. Numerical results corroborate the accuracy of the proposed expressions. These new formulas not only significantly improve the accuracy of the existing ones, but also lay the groundwork for the analysis of the beamwidth properties of the important case of 2-D LWAs.**

***Index Terms*—Leaky-wave antennas (LWAs), leaky waves, beamwidth, broadside radiation.**

I. Introduction and Motivation

LEAKY-wave antennas (LWAs) [1]–[3] are traveling-wave antennas [4] usually based on a waveguiding system, for which radiation occurs through the excitation of a partially-confined wave, viz., a *leaky wave*, propagating along a particular direction (here referred as the z-axis) and progressively *leaking* energy in free space. LWAs are typically classified as *one-dimensional* (1-D) or *two-dimensional* (2-D) LWAs, depending on whether the guiding structure is mainly 1-D or 2-D. Within the class of 1-D LWAs, a further distinction is made between 1-D *unidirectional* LWAs, for which radiation occurs from a leaky wave traveling along the positive z-axis, and 1-D *bidirectional* LWAs, for which radiation occurs from two identical leaky waves traveling along the $\pm z$-axis. Curiously, in spite of the one-dimensional nature of common leaky-waves, the physics of 1-D bidirectional LWAs is closer to that of 2-D LWAs than to 1-D unidirectional LWAs [2]. Therefore, a comprehensive description of the radiating properties of 1-D bidirectional LWAs is expected to allow for a thorough understanding of the radiating properties of 2-D LWAs as well.

Manuscript received XXX. xx^{xx}, xxxx

W. Fuscaldo and A. Galli are with the Department of Information Engineering, Electronics and Telecommunications, Sapienza University of Rome, 00184 Rome, Italy (email: {fuscaldo, galli}@diet.uniroma1.it).

D. R. Jackson is with the Department of Electrical and Computer Engineering, University of Houston, Houston, TX 77204-4005 USA (email: djackson@uh.edu).

In the past [1]–[3], the relevant radiating properties, such as the radiation efficiency, the pointing angle, and the half-power beamwidth (HPBW), of both 1-D unidirectional and 1-D bidirectional LWAs have theoretically been predicted in the asymptotic limit of an *infinite aperture* distribution, thus neglecting the effects of the *aperture truncation*. More recently, serious efforts have been made to improve these formulas for 1-D unidirectional LWAs [5], including the special case where the beam is scanned beyond the ordinary endfire condition [6], i.e., when $\beta > k_0$ (where k_0 is the vacuum wavenumber, and β is the phase constant of the propagating complex wavenumber $k_x = \beta - j\alpha$, being α the attenuation constant).

In these works [5], [6] the aperture truncation was finally accounted for and the accuracy of the beamwidth formulas was considerably improved as well. Specifically, a general formula for the evaluation of the beamwidth in 1-D unidirectional LWAs is derived in [5], which is accurate for any combination of phase constant, attenuation constant, and aperture length (where previous formulations are notably restricted to certain ranges [1]–[3]), provided that $\beta \leq k_0$. To account for cases where $\beta > k_0$, i.e., when the beam points at endfire but the phase constant is further increased to improve directivity [7], new formulas have been derived in [6] for describing the beamwidth and the sidelobe level of *endfire LWAs*.

However, these results [5], [6] only apply to 1-D unidirectional LWAs, whereas the beamwidth properties of either 1-D bidirectional LWAs or 2-D LWAs have been derived assuming *infinite* aperture distributions [8], [9]. The beam properties of finite-length 1-D bidirectional LWAs were discussed only in [10]. In particular, it was shown that, differently from the infinite-case, a 1-D bidirectional LWA of finite length radiates at broadside even beyond the ordinary *splitting-point* condition (i.e., when the beam maximum is pointed exactly at broadside). Although the novel splitting-condition for the finite-case was numerically found, no formulas were provided.

In this work, we first discuss the beam properties of infinite 1-D bidirectional LWAs in a novel fashion. Specifically, we generalize the definition of *broadside beam* as one for which the beam maximum may point off broadside, but the power density at broadside is within 3 dB of the maximum power density. We call the -3 dB point at broadside the *dual-beam* condition. Under this new definition, it is shown that a region exists for which a broadside beam is obtained, even beyond the splitting-point condition for infinite apertures. As a result, three different radiating regimes are clearly identified, whose boundaries are set by the splitting-point and the dual-beam conditions. Interestingly, the variation of these boundaries as the aperture truncation is accounted for is predicted by simple analytical formulas. Moreover, exact and approximate analytical

formulas for evaluating the beamwidth in the three different radiating regimes are provided for the *infinite-case* and the *finite-case*, respectively.

The paper is organized as follows. In Section II, radiation from 1-D bidirectional LWAs with finite apertures is briefly reviewed and conveniently cast in a suitable formalism. In Section III, analytical results for infinite-aperture 1-D bidirectional LWAs are shown to directly emerge from our new formulation. In Section IV analytical results for finite-aperture 1-D bidirectional LWAs are obtained and corroborated by numerical means in Section V. Section V also presents two realistic design applications using the new beamwidth formula, as well as an optimization of a Fabry-Perot cavity LWA using the new formula. Conclusions are drawn in Section VI.

II. Radiating properties of 1-D bidirectional LWAs

In this Section, we review the radiating properties of 1-D bidirectional LWAs as those depicted in Fig. 1. Basically, a bidirectional leaky wave is excited from the center $x = 0$ of a waveguiding system and travels towards the edges of the structure at $x = \pm L/2$ (L being the aperture length), where an absorbing material is usually put to avoid spurious radiation arising from multiple reflections.

Radiation is assumed to emanate from the upper aperture face (at $z = 0$ in Fig. 1). The mechanism of radiation (as well as the feed structure) may vary from one structure to another. For example, the structure may be a rectangular waveguide radiating from a longitudinal slot in one of the walls. It may also be a printed microstrip line radiating from periodic perturbations placed along the line, thus acting as a periodic LWA. In the following, we do not restrict our attention to a specific type of structure. However, we will always assume that the dominant contribution to radiation arises from a single leaky-wave field [11], [12], and thus the aperture field distribution can be modeled with an exponential function of the type $e^{-jk_x|x|}$, where $k_x = \beta - j\alpha$ is the propagation wavenumber of the radiating leaky-wave field.

Under these general assumptions, the radiated power density distribution $P(\theta)$ of a bidirectional LWA of length L is easily obtained by taking the modulus squared of the expression for the *space factor* (SF) reported in [2] (viz., $P(\theta) = |\mathrm{SF}|^2$). The definition of the following normalized variables

$$\begin{cases} l = k_0 L/2, \\ p = k_x L/2 = \beta L/2 - j\alpha L/2 = b - ja, \\ t = l \sin\theta, \end{cases} \tag{1}$$

where θ is the angle measured from the vertical z-axis to the longitudinal x-axis (thus $\theta = 0^\circ$ would correspond to broadside), allows for obtaining a compact expression

$$P(\theta) = \frac{L^2}{|t^2 - p^2|^2} \left| p - e^{-jp}(p\cos t + jt\sin t) \right|^2. \tag{2}$$

This equation will be used throughout the paper to derive the beamwidth properties of 1-D bidirectional LWAs in the most general case.

As can be inferred from Eq. (2), the radiation pattern exhibit two beams with maxima at $t = \pm p$. These two beams will be separate when $\beta \gg \alpha$ (in that case the two beams point at $\theta_p \simeq \pm \arcsin \beta/k_0$). However, at the *splitting-point condition*, when $\beta \simeq \alpha$ for an infinite aperture [8] (the case of a finite aperture will be considered later), these two beams will merge with each other at broadside (as shown in Fig. 1), thus producing a single broadside beam. This feature mainly motivates the interest in 1-D bidirectional LWAs [2] and is extensively explored in the next Sections. Specifically, in Section III we discuss cases for which 1-D bidirectional LWAs point off broadside and also derive the results for infinite apertures as asymptotic limits of Eq. (2).

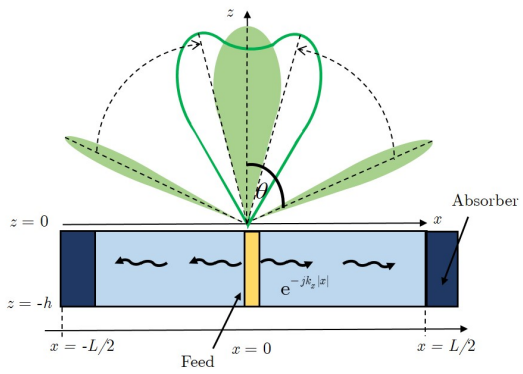

Fig. 1. A sketch of a 1-D bidirectional LWA of length L. The evolution of the radiation pattern as a function of the frequency is also reported, highlighting how the two beams merge at broadside in a single beam when the splitting-point condition is achieved.

III. Beamwidth properties of infinite 1-D bidirectional LWAs

In *infinite* 1-D bidirectional LWAs, the splitting-point condition always happens when $\beta = \alpha$ [8]; this suggests to distinguish the beamwidth properties of 1-D bidirectional antennas for cases where $\beta < \alpha$, $\beta = \alpha$, and $\beta > \alpha$. (It should be noted that an infinite aperture will never be realized in practice, but may serve as a good approximation for those cases where the radiation efficiency is very high, e.g., greater than 98%.)

A. Asymptotic evaluation of the beamwidth when $\beta < \alpha$

In the limit of an infinite aperture, i.e., $a \to \infty$, Eq. (2) yields:

$$P_\infty(\theta) = \lim_{a\to\infty} P(\theta) = \frac{L^2|p|^2}{|t^2 - p^2|^2}. \tag{3}$$

When $\beta < \alpha$ the beam points at broadside, although the radiated power density is no longer maximized in structures based on partially reflecting screens (PRSs) [8]. In this regime it is possible to normalize $P_\infty(\theta)$ to $P_\infty(0)$, and obtain the beamwidth equation:

$$\bar{P}_\infty(\Delta\theta_\mathrm{h}) = \lim_{a\to\infty} \bar{P}(\Delta\theta_\mathrm{h}) = \frac{|p|^4}{|p^2 - t_\mathrm{h}^2|^2} = \frac{1}{2}. \tag{4}$$

The angle $\Delta\theta_\mathrm{h}$ is the one-sided beamwidth (the angle from broadside to the -3 dB point), which is one half of the -3 dB beamwidth. Introducing the unitless variable $r = \beta/\alpha$, Eq. (4)

can be conveniently recast. After some algebra, we get a biquadratic equation whose roots are given by:

$$t_{\rm h} = \pm a\sqrt{r^2-1\pm\sqrt{2(r^4+1)}}. \tag{5}$$

Taking the positive determinations of the square roots (which corresponds to considering the right-side of the beamwidth with respect to the positive pointing angle), we get the sought expression of $\Delta\theta_{\rm h}$:

$$\Delta\theta_{\rm h} = \arcsin\sqrt{\hat\beta^2-\hat\alpha^2+\sqrt{2(\hat\beta^4+\hat\alpha^4)}} \tag{6}$$

where $\hat\beta = \beta/k_0 = b/l$ and $\hat\alpha = \alpha/k_0 = a/l$. In the small beamwidth approximation ($\Delta\theta_{\rm h} \ll 1$), Eq. (6) coincides with the well-known expression for the beamwidth of 2-D LWAs in the limit of an infinite aperture previously reported in [8]. From this equation it is readily found that, when β and α are independent, the beamwidth of an infinite 1-D bidirectional LWA for a given α is minimized for $\beta = 0$, for which we have

$$\Delta\theta_{\rm h}^{(\min)} = \hat\alpha\sqrt{-1+\sqrt{2}} \simeq 0.6436\hat\alpha. \tag{7}$$

While this remains true for the finite aperture-case (see Section IV), this condition no longer holds when β and α are related, as in PRS-type of structures [8]. In this case $\hat\beta\hat\alpha = C$, where C is a constant which accounts for the reflectivity of the PRS and the substrate losses. For PRS-based 1-D bidirectional LWAs with infinite apertures, the beamwidth is minimized for $r = 0.5176$ [8], for which we have

$$\Delta\theta_{\rm h}^{(\min)} \simeq 0.8556\hat\alpha. \tag{8}$$

On the other hand, when the antenna is finite, the value of r which minimizes the beamwidth will be a function of the radiation efficiency. This is a worthwhile aspect that will be discussed in a future investigation.

B. Asymptotic evaluation of the beamwidth when $\beta = \alpha$

When $\beta = \alpha$, a broadside beam is obtained for which the radiated power density is maximized when the LWA is a PRS-type of structure that is excited by a bidirectional dipole-like source [8]. In this case it is still possible to use Eq. (5), which for $r = \beta/\alpha = 1$ gives $t_{\rm h} = \sqrt{2}a$. Moreover, in the approximation of small beamwidth, $t_{\rm h} \simeq l\Delta\theta_{\rm h}$, this yields

$$\Delta\theta_{\rm h} = \sqrt{2}a/l = \sqrt{2}\hat\alpha, \tag{9}$$

in agreement with the result found in the literature for 2-D LWAs [1]–[3].

We recall here that the *splitting-point* condition is defined as the largest ratio $r_{\rm s}$ for which the beam maximum is still at broadside. For an infinite aperture, $r_{\rm s} = 1$. For finite apertures, the splitting point does not generally correspond to $r_{\rm s} = 1$, but it is a function of the radiation efficiency [10] (see Section IV). We therefore refer to $r_{\rm s,\infty} = 1$, as the splitting-point condition for infinite apertures.

C. Asymptotic evaluation of the beamwidth when $\beta > \alpha$

The case $\beta \gg \alpha$ is straightforward: the beamwidth properties are exactly the same for 1-D unidirectional LWAs and formulas are provided in any textbook about LWAs [1]–[3]. However, when β is just slightly greater than α, the two symmetric beams have merged together, forming an overall beam that no longer has a maximum at broadside (see Fig. 2). Hence, the usual definition of beamwidth could be ambiguous. We call the *dual-beam* condition the value $r_{\rm d}$ for which the main lobe has decreased to exactly -3 dB at broadside with respect to the beam maximum. As for the splitting-point condition, the dual-beam condition is generally a function of the efficiency (see Section IV), while for infinite apertures it corresponds to $r_{\rm d,\infty} \simeq 2.414$ as we show at the end of this Subsection.

When $r > 1$ the beam maximum is no longer at broadside, thus Eq. (5) can no longer be used. In order to get a beamwidth equation for split or dual beams, one would normalize $P_\infty(\theta)$ to the maximum $P_\infty(\theta_p)$, where θ_p is the angle of the beam peak. Since in an infinite bidirectional 1-D LWA θ_p is given by [2]

$$\theta_p = \arcsin\sqrt{\hat\beta^2-\hat\alpha^2}, \tag{10}$$

the beamwidth equation is obtained from Eq. (3) and reads

$$\left[t_{\rm h}^2-(b^2-a^2)\right]^2 = 4a^2b^2, \tag{11}$$

where $t_{\rm h} = l\sin(\theta_p\pm\Delta\theta_{\rm h})$. This biquadratic equation admits four solutions, which clearly represent two pairs of solutions symmetric to broadside. If one takes the positive determination for $t_{\rm h}$ (and hence for $\Delta\theta_{\rm h}$), the two solutions (that are no longer symmetric) identify the right-sided and left-sided -3 dB beamwidths with respect to the maximum on the right side as:

$$\Delta\theta_{\rm h,r} = +\arcsin\sqrt{\hat\beta^2-\hat\alpha^2+2\hat\alpha\hat\beta}-\theta_p, \tag{12}$$

$$\Delta\theta_{\rm h,l} = -\arcsin\sqrt{\hat\beta^2-\hat\alpha^2-2\hat\alpha\hat\beta}+\theta_p. \tag{13}$$

It may easily be verified that in the small beamwidth approximation ($\hat\alpha \ll 1$), Eqs. (6), (9), and (12) all agree for $\hat\beta = \hat\alpha$.

Clearly, the right-sided beamwidth (i.e., $\Delta\theta_{\rm h,r}$) always exists, whereas the left-sided beamwidth (i.e., $\Delta\theta_{\rm h,l}$) exists as long as $\hat\beta^2-\hat\alpha^2 > 2\hat\alpha\hat\beta$, or equivalently $r^2-2r-1 > 0$. The condition for the emergence of the left-sided beamwidth ($r^2-2r-1 = 0$) corresponds to the dual-beam condition for infinite apertures, and its asymptotic value is therefore

$$r_{\rm d,\infty} = 1+\sqrt{2} \simeq 2.414, \tag{14}$$

as mentioned at the beginning of this Subsection. When $r > r_{\rm d}$, the beamwidth is given by $\Delta\theta_{\rm h,r}-\Delta\theta_{\rm h,l}$. When $r < r_{\rm d}$, the beamwidth is given by $2\Delta\theta_{\rm h,r}$.

D. Evolution of the beam in infinite 1-D bidirectional LWAs

For $0 < r < r_{\rm d,\infty}$ an infinite 1-D bidirectional LWAs exhibits a single broadside beam (see Fig. 2). In particular, three different radiating regimes are easily recognized:

1) $0 < r < r_{\rm s,\infty}$;
2) $r_{\rm s,\infty} < r < r_{\rm d,\infty}$;
3) $r > r_{\rm d,\infty}$.

This article has been accepted for publication in a future issue of this journal, but has not been fully edited. Content may change prior to final publication. Citation information: DOI 10.1109/TAP.2019.2906014, IEEE Transactions on Antennas and Propagation

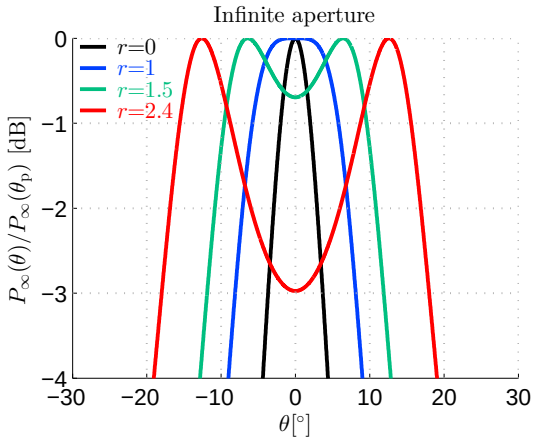

Fig. 2. (a) Radiation patterns of an infinite 1-D bidirectional LWA normalized to their maximum $P_\infty(\theta)/P_\infty(\theta_p)$ vs. θ for four different values of $r=\beta/\alpha$ ranging as $0 \le r \le r_{d,\infty}$ and $\hat{\alpha}=0.1$. As r increases beyond the splitting-point condition $r>1$, the beam is scalloped at broadside. However, as long as $r \le 2.414$ the power radiated at broadside has not decreased beyond -3 dB, and the beam can still be considered a single broadside beam.

In the first regime, we have a broadside beam (see, e.g., the black and blue curves in Fig. 2) that has no *scalloping* (i.e., exhibiting a local minimum at broadside). In this case, the double-sided beamwidth (HPBW) is given by:

$$\mathrm{HPBW} = 2\Delta\theta_\mathrm{h}, \tag{15}$$

with $\Delta\theta_\mathrm{h}$ given by Eq. (6).

In the second regime we have a split beam (see, e.g., the green and red curves in Fig. 2), but the amplitude at broadside is more than -3 dB above the level at the beam maximum, and therefore we have a *scalloped* beam, whose beamwidth is still given by Eq. (15), upon substitution of $\Delta\theta_{\mathrm{h,r}}$ in Eq. (12), assuming $\theta_\mathrm{p}=0$.

In the third regime, we can say that we truly have two different beams, and the beamwidth of each one is

$$\begin{aligned}\mathrm{HPBW} &= \Delta\theta_{\mathrm{h,r}}+\Delta\theta_{\mathrm{h,l}} \\ &= \arcsin\left(\hat{\alpha}\sqrt{r^2-1+2r}\right)-\arcsin\left(\hat{\alpha}\sqrt{r^2-1-2r}\right) \\ &\simeq \hat{\alpha}\left(\sqrt{r^2+2r-1}-\sqrt{r^2-2r-1}\right). \end{aligned} \tag{16}$$

The beamwidth is continuous as we transition from the first regime to the second

$$\lim_{r\to 1^+}\mathrm{HPBW} = \lim_{r\to 1^-}\mathrm{HPBW} = 2\arcsin\left(\hat{\alpha}\sqrt{2}\right) \tag{17}$$

but is discontinuous as we transition from the second regime to the third. Indeed, for $r \to r_{d,\infty}$, then $\Delta\theta_{\mathrm{h,l}} \to 0$, and thus the double-sided beamwidth suddenly drops by a factor of 2 (the central beam region, defined by the -3 dB points, suddenly becomes one-sided instead of two-sided). The relevant formulas of the HPBW (viz., double-sided beamwidth) for all the radiating regimes are conveniently summarized in Table I.

It is worth to stress here that Eq. (16) generalizes the formula for the beamwdith of infinite 1-D bidirectional LWA pointing off-broadside reported in [2]

$$\mathrm{HPBW} = 2\hat{\alpha}\sec\theta_\mathrm{p}, \tag{18}$$

which can easily be derived from Eq. (16) in the small beamwidth approximation and for $r \gg 1$. However, when the beam is not considerably small these formulas are rather inaccurate. Just to give some numbers, from Fig. 2 we note that the one-sided beamwidth for $r=2.4$ and $\hat{\alpha}=0.1$ is around $18°$. This is accurately predicted by Eq. (16), whereas the application of Eq. (18) along with Eq. (10) furnishes a value around $12°$, leading to an error of more than 30%.

IV. Beamwidth Properties of Finite 1-D Bidirectional LWAs

In this Section, we aim to extend the previous results for infinite 1-D bidirectional LWAs to the important case of *finite* 1-D bidirectional LWAs. This Section IV is divided in three Subsections. In Subsection IV-A, we show how the radiating properties of a finite-length 1-D bidirectional LWA change as r increases beyond the splitting-point and the dual-beam conditions, for different values of efficiencies. In Subsection IV-B, we discuss how the splitting-point and the dual-beam conditions change as the aperture truncation is accounted for. In particular, approximate formulas are obtained for evaluating both conditions as functions of the radiation efficiency. In Subsection IV-C, we derive an exact transcendental beamwidth equation for finite-length 1-D bidirectional LWA pointing at broadside. Its numerical solution will be the object of Section V.

A. Evolution of the beam in finite 1-D bidirectional LWAs

The evolution of the beam for $0 \le r < 2.414$ of an infinite 1-D bidirectional LWA has been reported in Fig. 2. In order to inspect what happens when the lateral truncation is accounted for (finite L), we report in Figs. 3(a)-(h) the same patterns of Fig. 3(a), but for radiation efficiencies ranging from $e_\mathrm{r}=99.9\%$ to $e_\mathrm{r}=80\%$, corresponding to antenna lengths ranging from 11λ, to 2.5λ, assuming $\hat{\alpha}=0.1$. We note that, throughout the paper, the radiation efficiency is defined as $e_\mathrm{r}=1-\exp(-2a)=1-\exp(-2\pi\hat{\alpha}L/\lambda)$, as we are neglecting material losses.

TABLE I
Formulas for the HPBW and the beam angle in the different radiating regimes for infinite 1-D bidirectional LWAs.

Radiating regime	HPBW formula	Beam angle
$0<r<1$	$2\arcsin\left(\hat{\alpha}\sqrt{r^2-1+\sqrt{2(r^4+1)}}\right)$	0
$r=1$	$2\arcsin\left(\hat{\alpha}\sqrt{2}\right)$	0
$1<r<1+\sqrt{2}$	$2\arcsin\left(\hat{\alpha}\sqrt{r^2-1+2r}\right)$	$\arcsin\hat{\alpha}\sqrt{r^2-1}$
$r>1+\sqrt{2}$	$\arcsin\left(\hat{\alpha}\sqrt{r^2-1+2r}\right)-\arcsin\left(\hat{\alpha}\sqrt{r^2-1-2r}\right)$	$\arcsin\hat{\alpha}\sqrt{r^2-1}$

This article has been accepted for publication in a future issue of this journal, but has not been fully edited. Content may change prior to final publication. Citation information: DOI 10.1109/TAP.2019.2906014, IEEE Transactions on Antennas and Propagation

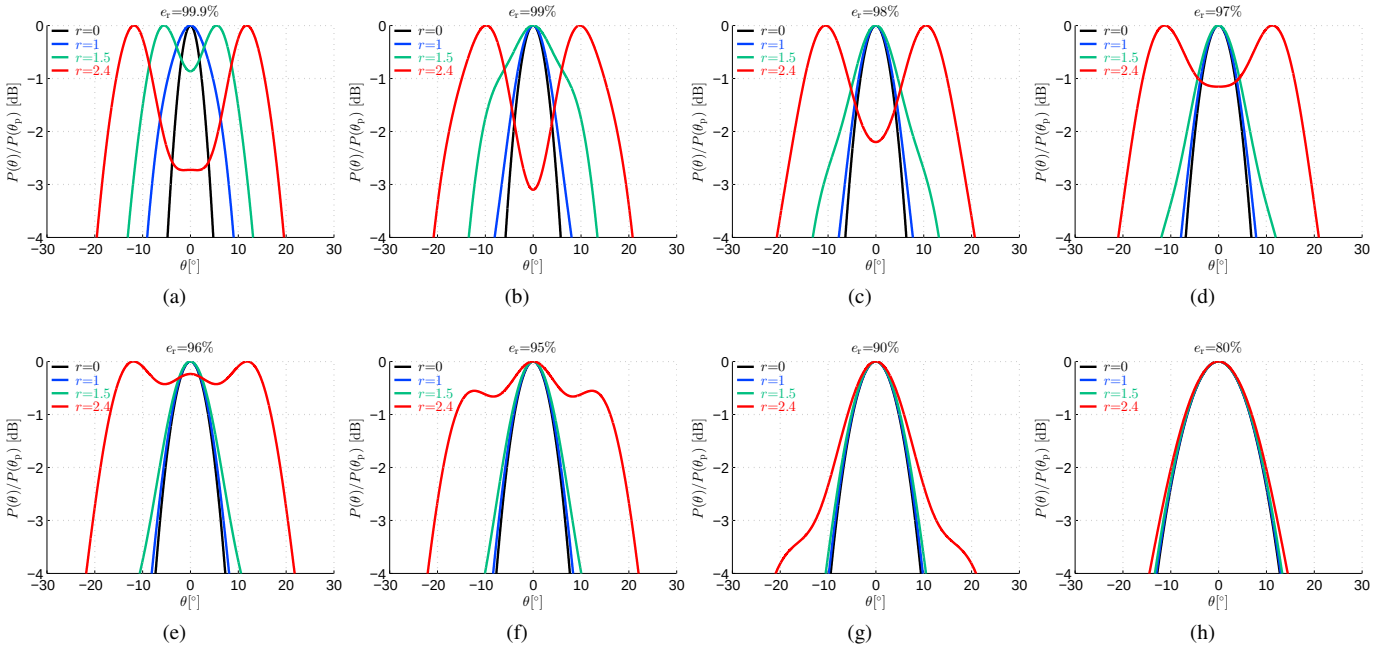

Fig. 3. (a)-(h) As in Fig. 2 but for finite-length 1-D bidirectional LWAs with different radiation efficiencies ranging from $e_{\rm r} = 99.9\%$ to 80%. For $\hat{\alpha} = 0.1$ this would correspond to antenna lengths ranging from 11λ, to 2.5λ, respectively. It should be noted that, in the finite case, $\theta_{\rm p}$ is no longer given by Eq. (10), but it is numerically evaluated from Eq. (2).

As already shown in [10], as the efficiency decreases a broadside beam (i.e., when the beam maximum is directed exactly at broadside) is obtained even for $r > 1$. Specifically, $r_{\rm s}$ is a decreasing function of the efficiency as confirmed by Figs. 3(a)-(h). In particular, for efficiencies of 95% and lower (see Figs. 3(f)-(h)), r_s is certainly greater than 2.4, while for efficiencies as high as 96% or 99.9%, r_s is lower than 2.4, or 1.5, respectively (see the scalloping of the beam at broadside for the red curve in Fig. 3(e) and for the green curve in Fig. 3(a), respectively). We also note that, as the efficiency decreases beyond 90%, r mildly affects the pattern shape.

Conversely, the dual-beam condition (i.e., when the power density radiated at broadside is 3 dB lower than the power density at the beam peak) seemingly does not have a monotonic behavior, being reached for $r = 2.4$ when $e_{\rm r} = 99\%$ (see the red curve Fig. 3(b)), but still not reached for $r = 2.4$ when $e_{\rm r} = 99.9\%$ (see the red curve in Fig. 3(a)). These observations further motivate the need of accurate formulas for the evaluation of both $r_{\rm s}$ and $r_{\rm d}$ as functions of $e_{\rm r}$. These aspects are the object of the next Subsection IV-B.

B. Splitting-point and dual-beam conditions

As previously shown, for finite-length 1-D bidirectional LWAs the splitting-point condition is no longer given by the condition $r_{\rm s} = 1$ but it is a function of the radiation efficiency $e_{\rm r}$. Nevertheless, $r_{\rm s} = 1$ represents a lower bound to the splitting-point condition (asymptotically achieved for infinite apertures), thanks to the monotonic behavior of $r_{\rm s}(e_{\rm r})$.

In [10] the value of $r_{\rm s}$ as a function of $e_{\rm r}$ was found numerically for efficiencies ranging from 70% to 99%, thus covering most practical LWA designs. However, no *formulas* have been proposed so far. However, for design purposes it would be really helpful to have an approximate formula for the *splitting-point condition*, especially over an extended range of efficiencies. To this purpose, we have numerically searched for the value of $r_{\rm s}$, which is the largest value of r that satisfies the equation $P(0) = \max P(\theta)$, for $0.2 < a < 5$ (thus covering efficiencies in the range $33\% < e_{\rm r} < 99.995\%$), and fit $r_{\rm s}$ as a function of a with a suitable fitting scheme:

$$r_{\rm s}(a) = \tanh(u_1 a) + u_2 \frac{1-\tanh(u_4 a)}{a^{u_3}}, \tag{19}$$

with fitting parameters u_i, $i = 1, 2, 3, 4$:

$$u_1 = 1.221, \quad u_2 = 4.168, \quad u_3 = 0.935, \quad u_4 = 0.326.$$

Numerical results for $r_{\rm s}$ as a function of a, are shown in Fig. 4(a). This choice leads to a mean absolute percent error (MAPE) around 2%. The accuracy of the approximation can also be checked in Fig. 4(b), where the numerical solution (in solid black line) of $r_{\rm s}$ and the fitting scheme (in circles) from Eq. (19) are almost overlapped. Note that the numerical results agree well with those obtained in [10] for the restricted range $0.6 \le a \le 2.3$ (corresponding to $70\% < e_{\rm r} < 99\%$) that is presented in [10] (compare Fig. 4(b) with Fig. 2 in [10]).

The same approach can be applied to derive an approximate formula for the *dual-beam condition* in the *finite-aperture* case. In this case, however, numerical solutions were not previosuly derived in the available literature. We therefore numerically searched for the value $r_{\rm d}$ that satisfies the equation $P(0) = P_{\max}/2$, for $0.2 < a < 5$, where $P_{\max} = \max P(\theta)$, and fit $r_{\rm d}$ as a function of a with the following fitting scheme:

$$r_{\rm d}(a) = \left[r_{\rm d,\infty} + \frac{1}{2[1+(a-2.8)^2]}\right]\left[\frac{1+\tanh(a-2.8)}{2}\right] + \left[v_1 + \frac{v_3}{(5a)^{v_2}}\right]\left[\frac{1+\tanh(2.8-a)}{2}\right] \tag{20}$$

This article has been accepted for publication in a future issue of this journal, but has not been fully edited. Content may change prior to final publication. Citation information: DOI 10.1109/TAP.2019.2906014, IEEE Transactions on Antennas and Propagation

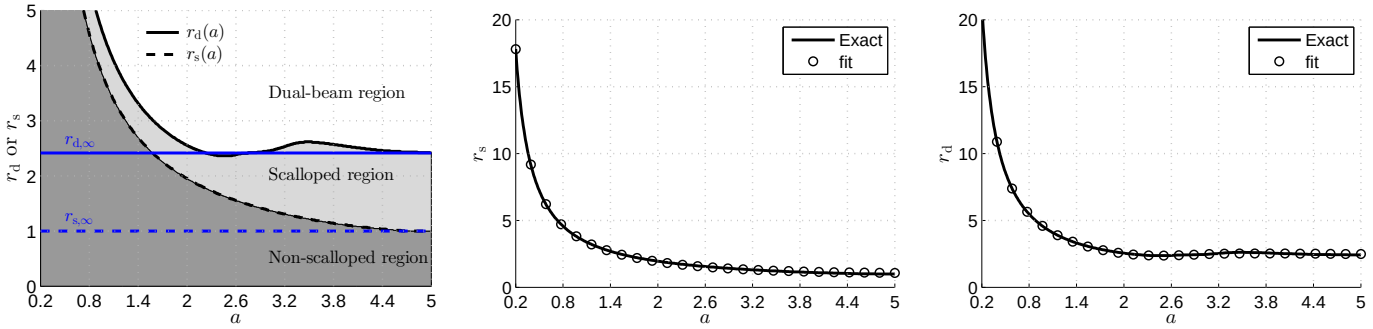

(a) (b) (c)

Fig. 4. (a) Splitting-point $r_{\rm s}$ (black dashed line) and dual-beam $r_{\rm d}$ (black solid line) conditions vs. a in the range $0.2 \leq a \leq 5$ (corresponding to efficiencies $30\% < e_{\rm r} < 99.99\%$). The $r_{\rm s}$ and $r_{\rm d}$ curves delimit the boundaries between the first (dark-grey shaded area) and second (light-grey shaded area) regime, and between the second and the third regime (white area), respectively, for finite-length 1-D bidirectional LWAs. Both $r_{\rm s}$ and $r_{\rm d}$ asymptotically converge to $r_{\rm s,\infty} = 1$ (blue dashed line), and $r_{\rm d,\infty} = 1+\sqrt{2}$ (blue solid line), respectively, as has been found for the infinite aperture case. (b) $r_{\rm s}$ vs. a (black solid line) and its fitting by means of Eq. (19) (black circles). (c) $r_{\rm d}$ vs. a (black solid line) and its fitting by means of Eq. (20) (black circles).

with fitting parameters v_i, $i = 1, 2, 3$:

$$v_1 = 0.54, \quad v_2 = 1.03, \quad v_3 = 20.81.$$

This choice leads to a mean absolute percent error (MAPE) around 1%. The accuracy of the approximation can also be checked in Fig. 4(c).

At this point it is worthwhile to comment on Fig. 4(a), where the splitting-point $r_{\rm s}(a)$ and the dual-beam $r_{\rm d}(a)$ curves are shown in a single plot. It is seen that $r_{\rm d}(a) > r_{\rm s}(a)$, $\forall a$, as expected from the definitions of splitting-point and dual-beam conditions. Interestingly, for $2.2 < a < 2.8$, corresponding to efficiencies $98.7\% < e_{\rm r} < 99.7\%$, we note that $r_{\rm d} < 1+\sqrt{2}$, reaching a minimum value of 2.36, and thus explaining the result of Fig. 3(b), where for $r = 2.4$ the value at broadside is less than -3dB for $e_{\rm r} = 99\%$. Furthermore, Fig. 4(a) shows us that, even for finite apertures, it is possible to distinguish three radiating regimes (as in Subsection III-D for infinite apertures), whose boundaries are dictated by $r_{\rm s}(a)$ (between the first and the second regime) and by $r_{\rm d}(a)$ (between the second and the third regime). As expected, these boundaries asymptotically converge to the values found for the infinite-aperture case, i.e., $r_{\rm s,\infty}$, and $r_{\rm d,\infty}$, respectively.

To further corroborate the splitting-point and the dual-beam conditions for finite apertures, as well as the respective fitting schemes, we show in Fig. 5 the evolution of the normalized radiation patterns for $r = r_{\rm s,\infty}$, $r = r_{\rm d,\infty}$, $r = r_{\rm s}$, $r = r_{\rm d}$, and $r = 1.1r_{\rm d}$ for an efficiency of 90% (as it is one of the most common choice in LWA design). As is shown in Fig. 5, when either $r = 1$ or $r = 1+\sqrt{2}$, the beam still points at broadside due to the effect of the aperture truncation. However, when $r = r_{\rm s}(a_0)$ and $r = r_{\rm d}(a_0)$ (where $a_0 \simeq 1.15$, corresponding to $e_{\rm r} = 90\%$) the power at broadside is at the same level of that at the beam maximum, and at a -3 dB of the beam maximum, respectively. It is interesting to note that when $r = r_{\rm s}(a)$ in the finite aperture case (the green curve in Fig. 5) , the beam shows scalloping. For the infinite aperture case, the beam does not show scalloping when $r = r_{\rm s,\infty} = 1$. Finally, as r increases beyond $r_{\rm d}(a)$ the beam is definitely split in two distinguished beams pointing off broadside, thus corroborating the boundaries between the radiating regimes shown in Fig. 4(a).

The next Subsection IV-C is entirely devoted to the derivation of an exact beamwdith equation for finite-length 1-D bidirectional LWAs operating in the first and second regimes, i.e., when a beam, either scalloped or not, still points at broadside.

C. Beamwidth equation

Here we are interested in deriving an exact beamwidth equation for finite-length 1-D bidirectional LWAs radiating at broadside. As a consequence, for the first regime (i.e., $0 \leq r \leq r_{\rm s}(a)$), it is useful to normalize $P(\theta)$ (see Eq. (2)) to the power density radiated at broadside $P(0)$. Upon normalization to $P(0)$, the one-sided half-power beamwidth $\Delta\theta_{\rm h}$ is found by equating $\bar{P}(\Delta\theta_{\rm h}) = P(0)/2$ and solving for the roots of the resulting transcendental equation:

$$2|p|^2 \left|p - e^{-jp}(p\cos t_{\rm h} + jt_{\rm h}\sin t_{\rm h})\right|^2 - \left|p^2 - t_{\rm h}^2\right|^2 \left|1 - e^{-jp}\right|^2 = 0. \tag{21}$$

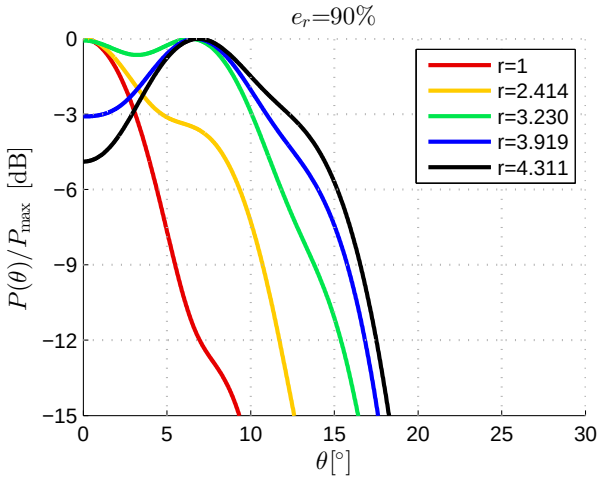

Fig. 5. Radiation patterns of a finite 1-D bidirectional LWA normalized to their maximum $P(\theta)/P_{\rm max}$ vs. θ for $r = \beta/\alpha \in \{r_{\rm s,\infty}, r_{\rm d,\infty}\, r_{\rm s}(a), r_{\rm d}(a), 1.1r_{\rm d}(a)\}$ when $a = a_0 \simeq 1.15$ (corresponding to $e_{\rm r} = 90\%$) for an antenna length of $L = 10\lambda$ (corresponding to $\hat{\alpha} \simeq 0.037$).

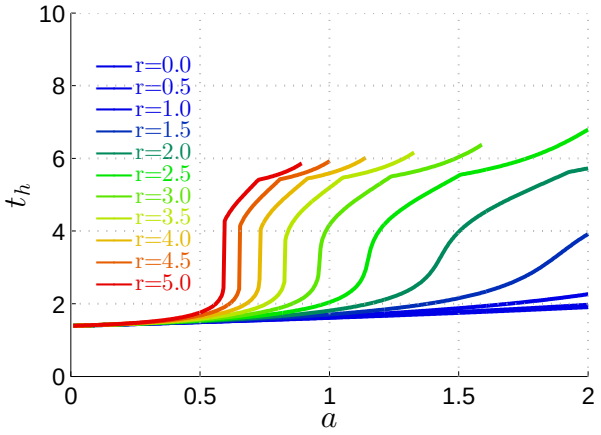

(a)

Fig. 6. (a) $t_{\rm h}$ vs. a in the range $0 < a \leq 2$ for r going from 0 to 5 (solid lines shade from blue to red). The curves are interrupted according to the dual-beam condition, i.e., for each r, the plot stops at the value of a for which $r = r_d(a)$ (as given in Fig. 4(a)).

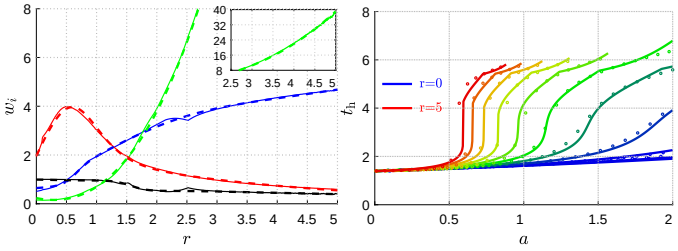

(a) (b)

Fig. 7. (a) Fitting coefficients w_1, w_2, w_3, and w_4 vs. r (in blue, green, red, and black solid lines, respectively). Their interpolations through Eq. (26) are shown in colored dashed lines. The asymptotic behaviors of w_2 (green solid line) and its interpolation (green dashed line) are shown in the inset for $2.5 \leq r \leq 5$. (b) $t_{\rm h}$ vs. a in the range $0 < a \leq 2$ for r going from 0 to 5 (solid lines shade from blue to red). Their interpolation through the fitting scheme given by Eqs. (25)-(26) is reported in small colored circles.

where $t_{\rm h} = l\sin(\Delta\theta_{\rm h})$. We note here that, for a uniform *constant aperture distribution*, i.e., for $a \to 0$ (therefore $p \to 0$, since we are assuming broadside radiation) Eq. (21) reduces to $t_{\rm h}^2 = 2\sin^2 t_{\rm h}$, whose numerical solution is $t_{\rm h} = 1.3915$, and thus, for small beamwidths,

$$\Delta\theta_{\rm h} = 1.3915/l \simeq 0.8859/(L/2\lambda), \tag{22}$$

in agreement with the results obtained by Oliner for a 1-D unidirectional LWA of length $L/2$ with a constant aperture field [1]. Incidentally, we notice that $t_{\rm h} = 1.3915$ is the same constant appearing in the beamwidth expression for uniform amplitude and uniform spacing 1-D broadside arrays [13]. This is fully consistent with the fact that a 1-D uniform array with constant spacing can be thought of as a discrete version of the 1-D LWA with a uniform aperture distribution.

Equation (21) is the sought exact beamwidth equation for 1-D bidirectional LWAs in the first regime. It is clear from Eq. (21) that $t_{\rm h}$ is a function of the single complex parameter p. Equivalently, $t_{\rm h}$ is a function of the parameters r and a. We therefore have [according to the definition of $t_{\rm h}$ right after Eq. (21)]:

$$\Delta\theta_{\rm h}(a, r, l) = \arcsin\left[t_{\rm h}(a; r)/l\right]. \tag{23}$$

Conversely, in the second radiating regime (i.e., for $r_{\rm s}(a) \leq r < r_{\rm d}(a)$), the beam exhibits a local minimum at broadside that is within 3 dB of the peak. As a result, the problem of evaluating its beamwidth generally requires the numerical solution of a beamwidth equation of the type

$$P(t_{\rm h}) - P_{\rm max}/2 = 0, \tag{24}$$

where $P_{\rm max}$ is a function of r and a. Note that Eq. (21) is a particular case of Eq. (24) when $P_{\rm max} = P(0)$. In any case, an efficient method to get an approximate analytical expression for $\Delta\theta_{\rm h}$ is to fit the numerical solutions $t_{\rm h}$ of either Eq. (21) or Eq. (24) with a suitable fitting scheme, and then use the resulting analytical formula for $t_{\rm h}$ in Eq. (23). This approach has already been performed in [5], [6] for finite-length 1-D *unidirectional* LWAs scanning from broadside to *ordinary* endfire ($\beta = k_0$) [5], and beyond ordinary endfire ($\beta > k_0$) [6]. The extension of this approach to finite-length 1-D *bidirectional* LWAs is the object of the next Section V.

V. Numerical Results for Beamwidth

In this Section, we aim to extend the previous results on the beamwidth for infinite 1-D bidirectional LWAs (see Section III) to the important case of *finite* 1-D bidirectional LWAs. Since the main interest in practical 1-D bidirectional LWAs regards those that radiate around broadside, we will focus our analysis to the first and second regimes. The third regime, i.e., the case of a dual-beam scanning off-broadside, is briefly discussed at the end of this Section, to complete the picture.

As we have seen in Subsection IV-B, in a finite 1-D bidirectional LWA, the boundaries of the radiating regimes change as the radiation efficiency changes. However, practical designs of LWAs rarely exceed radiation efficiencies greater than 98%, and thus the results in this Section V are limited to $a \leq 2$. As can be seen in Fig. 4(a), for $a > 0.8$ (i.e., for efficiencies higher than 80%) the condition $r = 5$ represents an upper-bound for the boundary between the second and the third regime. This means that when dealing with broadside beams (the most practical case of interest) and practical efficiencies (greater than 80%), we can limit the region of interest to $r \leq 5$. The numerical solution of Eq. (24) and its fitting scheme will thus be performed over the range $0 < a \leq 2$ and $0 \leq r \leq 5$, using the (r, a) combinations that correspond to a broadside beam (lying below the topmost curve Fig. 4(a)).

The numerical solution of Eq. (24) is reported in Fig. 6 where a family of r-curves (for $0 \leq r \leq 5$ the curves shade from blue to red) showing $t_{\rm h}$ vs. a is represented in the range $0 < a \leq 2$. We should note that by means of Fig. 4(a) we can also predict, for each value of r: *i)* the value a_d for which $r = r_d(a_d)$ and the beam is splitting in a dual-beam (thus, for $a > a_d$ the plot is not shown because the transition from the second and the third regime is discontinuous (see Subsection III-D)); *ii)* the value a_s for which $r = r_s(a_s)$ and the beam is scalloping (thus, for $a > a_s$ we note a *cusp* point because the transition from the first and the second regime is continuous, but its derivative not (see Subsection III-D)). For example, for $r = 3$ we evidently have $a_s \simeq 1.2$, as reflected by the *cusp* around

This article has been accepted for publication in a future issue of this journal, but has not been fully edited. Content may change prior to final publication. Citation information: DOI 10.1109/TAP.2019.2906014, IEEE Transactions on Antennas and Propagation

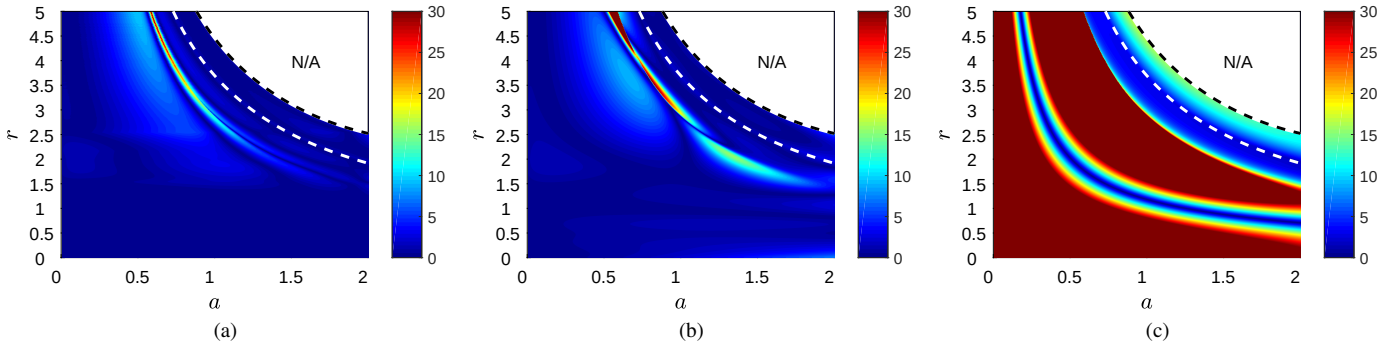

Fig. 8. Contour plots of the absolute percent error (APE) vs. a and r for (a) the fitting scheme [Eq. (25)], (b) the numerically-evaluated fitting scheme [Eq. (25)] with coefficients given by Eq. (26), and (c) for the infinite case [Eq. (5)]. The white dashed line represents the splitting-point condition $r(a) = r_s(a)$ [Eq. (19)], i.e., the boundary between the first and the second radiating regimes, whereas the black dashed line represents the dual-beam condition $r(a) = r_d(a)$ [Eq. (20)], i.e., the boundary between the second and the third radiating regimes. Accordingly, the region delimited by the white dotted line, and the upper-right corner corresponds to the dual-bem region; thus the beamwidth and consequently its APE is not calculated therein.

that point, and $a_d \simeq 1.6$, as reflected by the termination of the curve at that point (see the corresponding r-curve in Fig 6).

As is seen, the parameter r strongly affects the behavior of $t_{\rm h}(a)$ (see Fig. 6), so that it is not possible to find a simple fitting function for $t_{\rm h}(a)$. This fact would suggest a search for a family of r-parametric fitting functions of $t_{\rm h}(a;r)$ having r as a parameter. For any value of r this class of functions will be characterized by a different set of parameters that depends only on r. This will result in a final parametric formula $t_{\rm h}(a;r)$:

$$t_{\rm h} = t_{\rm h,0} + \frac{w_1 a^{w_4}}{2}\left\{1+\frac{2}{\pi}\arctan\left[\frac{\pi w_2}{2}(a-w_3)\right]\right\}, \qquad (25)$$

where $t_{\rm h,0} = 1.3915$ is the asymptotic value $t_{\rm h,0} = \lim_{a\to 0} t_{\rm h}$ of a uniform distribution (see Section IV-C), whereas w_i for $i = 1, 2, 3, 4$ are fitting coefficients whose values depend on r as reported in Fig. 7(a). For any value of r in the range $0 \le r \le 5$, w_i for $i = 1, 2, 3, 4$ are computed to get the best fit to $t_{\rm h}(a;r)$ (see solid lines in Fig. 7(a)). However, in order to have a fully analytical expression for $t_{\rm h}(a;r)$, the w_i coefficients have to be fit as functions of r. A remarkable accuracy is obtained using the following fitting schemes:

$$\begin{aligned}
w_1(r) =& \left[0.5+w_{11}r\left(\frac{1+\tanh[w_{12}(r-0.6)]}{2}\right)\right] \\
&\times\left(\frac{1-\tanh[w_{13}(r-2.5)]}{2}\right)+(2.715+0.39r) \\
&\times\left(\frac{1+\tanh[w_{14}(r-2.5)]}{2}\right), \\
w_2(r) =& w_{21}+w_{22}r+w_{23}r^2+w_{24}r^3 \\
w_3(r) =& (1.94+w_{31}r)\left(\frac{1-\tanh[w_{32}(r-0.7)]}{2}\right) \\
&+(w_{33}e^{-w_{34}r})\left(\frac{1+\tanh[w_{32}(r-0.7)]}{2}\right), \\
w_4(r) =& (0.9921-0.0633r)\left(\frac{1-\tanh[w_{42}(r-w_{41})]}{2}\right) \\
&+(0.6676-0.0548r)\left(\frac{1+\tanh[w_{43}(r-w_{41})]}{2}\right), \qquad (26)
\end{aligned}$$

where all the coefficients w_{ij} for $i = 1, 2, 3, 4$ and $j = 1, 2, 3, 4$ have been reported in Table II. The interpolation of $w_i(r)$ through Eq. (26) is reported in dashed lines in Fig. 7(a), while the final interpolating curves of $t_{\rm h}(a;r)$ through both Eqs. (25) and (26) are reported in small colored circles in Fig. 7(b).

TABLE II
VALUES OF THE FITTING COEFFICIENTS FOR $w_1(r)$, $w_2(r)$, $w_3(r)$, AND $w_4(r)$.

w_{ij}	$j=1$	$j=2$	$j=3$	$j=4$
$i=1$	1.2044	4.5274	0.6020	0.5440
$i=2$	0.2345	-0.5130	0.8035	0.1704
$i=3$	5.5873	1.9710	2.3778	0.2925
$i=4$	1.5728	2.9941	2.0388	-

In order to better highlight the accuracy of the proposed fitting schemes we have evaluated the absolute percent error (APE) between the numerical solution of $t_{\rm h}$ and both Eq. (25) with numerical coefficients [see Fig. 8(a)], and Eq. (25) with coefficients provided by Eq. (26) [see Fig. 8(b)]. Indeed, the slight differences between Figs. 8(a) and (b) confirm us that the error introduced by Eq. (26) is small. In general, except for a very small region where the APE reaches values around 10%, the error is rather small, leading to a MAPE as small as 1.5%. Note that the white dashed line in Figs. 8(a)-(c) delimits the boundary between the first and the second radiating regime. Remarkably, the APE is less than 5%, even in that region.

Furthermore, in Fig. 8(c) we have evaluated the APE when $t_{\rm h}$ is calculated by means of Eq. (5), i.e., when an infinite aperture is considered. As shown, the APE is basically higher than 30% over the entire range (leading to a MAPE of 31.3%), reaching peak values of 100% of error. This makes impractical the use of this formula for a correct estimation of the beamwidth 1-D bidirectional LWA of any length, operating between the first and the second regime, thus motivating the introduction of Eq. (25) and Eq. (26), in place of Eq. (5). As a result, the final formula for the one-sided beamwidth $\Delta\theta_{\rm h}$ of a *finite-length* 1-D bidirectional LWA of length L takes the following form:

$$\begin{aligned}
\Delta\theta_{\rm h} =& \arcsin\left\{\frac{2.783}{k_0 L}+\frac{w_1(r)}{\pi}\left(\frac{\hat{\alpha}k_0 L}{2}\right)^{w_4(r)}\right. \\
&\left.\times\left[\frac{\pi}{2}+\arctan\left(\frac{\pi w_2(r)}{2}\left(\frac{\hat{\alpha}k_0 L}{2}-w_3(r)\right)\right)\right]\right\}, \qquad (27)
\end{aligned}$$

with $w_1(r)$, $w_2(r)$, $w_3(r)$, and $w_4(r)$ given by Eq. (26) with coefficients w_{ij} given in Table II. This formula accounts for

This article has been accepted for publication in a future issue of this journal, but has not been fully edited. Content may change prior to final publication. Citation information: DOI 10.1109/TAP.2019.2906014, IEEE Transactions on Antennas and Propagation

TABLE III
COMPARISON AMONG VALUES OF THE HPBW ($2\Delta\theta_{\rm h}$) IN DEGREES.

$r=3$	$\hat{\alpha}=0.1$			$\hat{\alpha}=0.05$			$\hat{\alpha}=0.01$		
$\beta=3\alpha$	Infinite	Finite	Fit	Infinite	Finite	Fit	Infinite	Finite	Fit
$e_{\rm r}=50\%$	54.28	50.72	49.82	26.39	24.73	24.32	5.23	4.91	4.83
$e_{\rm r}=75\%$	54.28	28.58	26.68	26.39	14.18	13.25	5.23	2.83	2.64
$e_{\rm r}=90\%$	54.28	52.55	52.70	26.39	25.58	25.65	5.23	5.07	5.09
$r=2.414$	$\hat{\alpha}=0.1$			$\hat{\alpha}=0.05$			$\hat{\alpha}=0.01$		
$\beta=2.414\alpha$	Infinite	Finite	Fit	Infinite	Finite	Fit	Infinite	Finite	Fit
$e_{\rm r}=50\%$	42.32	50.39	50.24	20.79	24.58	24.51	4.14	4.88	4.87
$e_{\rm r}=75\%$	42.32	27.24	26.43	20.79	13.52	13.13	4.14	2.70	2.62
$e_{\rm r}=90\%$	42.32	25.47	28.64	20.79	12.66	14.21	4.14	2.53	2.83
$r=1.5$	$\hat{\alpha}=0.1$			$\hat{\alpha}=0.05$			$\hat{\alpha}=0.01$		
$\beta=1.5\alpha$	Infinite	Finite	Fit	Infinite	Finite	Fit	Infinite	Finite	Fit
$e_{\rm r}=50\%$	25.13	50.04	50.18	12.49	24.42	24.48	2.49	4.85	4.86
$e_{\rm r}=75\%$	25.13	26.17	26.09	12.49	13.00	12.96	2.49	2.59	2.59
$e_{\rm r}=90\%$	25.13	17.97	17.94	12.49	8.96	8.94	2.49	1.79	1.79
$r=1$	$\hat{\alpha}=0.1$			$\hat{\alpha}=0.05$			$\hat{\alpha}=0.01$		
$\beta=\alpha$	Infinite	Finite	Fit	Infinite	Finite	Fit	Infinite	Finite	Fit
$e_{\rm r}=50\%$	16.26	49.93	49.94	8.11	24.36	24.37	1.63	4.84	4.84
$e_{\rm r}=75\%$	16.26	25.85	25.82	8.11	12.84	12.82	1.63	2.56	2.56
$e_{\rm r}=90\%$	16.26	17.05	16.97	8.11	8.50	8.46	1.63	1.70	1.69
$r=0.5$	$\hat{\alpha}=0.1$			$\hat{\alpha}=0.05$			$\hat{\alpha}=0.01$		
$\beta=\alpha/2$	Infinite	Finite	Fit	Infinite	Finite	Fit	Infinite	Finite	Fit
$e_{\rm r}=50\%$	9.65	49.86	50.11	4.82	24.33	24.45	0.96	4.83	4.85
$e_{\rm r}=75\%$	9.65	25.67	25.86	4.82	12.76	12.85	0.96	2.55	2.56
$e_{\rm r}=90\%$	9.65	16.62	16.96	4.82	8.29	8.36	0.96	1.66	1.67

any combination of $\hat{\alpha}$, r, and L, in the range $0 \leq r \leq 5$, and for efficiencies up to 98%.

To further corroborate the need for Eq. (27), we have provided in Table III the values of the two-sided half-power beamwidth HPBW (defined as $2\Delta\theta_{\rm h}$) calculated with the formulas for infinite apertures [i.e., Eq. (6)] and compared with those calculated with the formulas provided in this work for finite apertures (i.e., Eq. (23) with $t_{\rm h}$ calculated either numerically, labeled as 'Finite', or using the fitting scheme, i.e., Eqs. (26)-(27), labeled as 'Fit'). The results are reported for the relevant cases of efficiencies $e_{\rm r}=50\%$, 75%, 90%, $\hat{\alpha}=0.1, 0.05, 0.01$, and $r=0.5$, 1, 1.5, 2.414, 3 (for $r=3$ and $e_r \leq 95\%$ we still have broadside beams, see Fig. 4(a)). Note that, the aperture length L is assumed to change for any value of $\hat{\alpha}$ to guarantee a certain value of $e_{\rm r}$ through the given relation $e_{\rm r}=1-\exp\left(-2\hat{\alpha}\pi L/\lambda\right)$ (e.g., for $\hat{\alpha}=0.05$ and $e_{\rm r}=50\%$, 75%, 90%, we have $L/\lambda=2.2$, 4.4, 7.4).

As shown in Table III, formulas for the infinite aperture case when $r=1$ are able to provide a reasonable estimation of the beamwidth only for efficiencies greater than 90% (the results asymptotically converge to the correct result for higher efficiencies). When the efficiency is lower than $e_{\rm r}=90\%$ the infinite-length formula can no longer be retained as a valuable tool for the beamwidth evaluation. This is especially true for all the other cases, i.e., $r \neq 1$, where the infinite-length formula leads to considerable errors even for $e_{\rm r}=90\%$. An exception is represented by the case $e_{\rm r}=75\%$ and $r=1.5$, where results for the infinite case have the same accuracy of the new formulas. However, this would happen only for specific combinations of r and $e_{\rm r}$, where Eq. (25) 'accidentally' has a low APE as confirmed by Fig. 8(c). In general, the results in Table III highlight the need of the formulas proposed here for a correct evaluation of the beamwidth in practical designs of 1-D bidirectional LWAs.

To illustrate one use of the new beamwidth formula, we will consider two design examples. We take two different 1-D bidirectional PRS types of LWA structure. The first example is one of a substrate-superstrate leaky-wave antenna (SS-LWA) [14] of length $L=6\lambda$. The dielectric substrate and superstrate have permittivities $\varepsilon_{\rm r1}=2.1$ (teflon) and $\varepsilon_{\rm r2}=50$ (ceramic), and thicknesses $h_1=\lambda/(2\sqrt{\varepsilon_{\rm r1}})$ and $h_2=\lambda/(4\sqrt{\varepsilon_{\rm r2}})$. (In [14], the LWA was a 2-D LWA excited by a dipole source at the center. Here we assume that a 1-D bidirectional LWA is formed from the same substrate-superstrate, with an electric field inside the cavity that is in the y direction (see Fig. 1). The feed could be, for example, a horizontal probe in the y direction that excites the cavity. The pattern of the 1-D bidirectional LWA is thus the same as the H-plane pattern of the 2-D LWA.) The superstrate in a SS-LWA acts as a PRS, and thus the normalized phase and attenuation constants must obey the hyperbolic condition $\hat{\beta}\hat{\alpha}=r\hat{\alpha}^2=C$, where C is a constant determined by the PRS properties [8]. In the case of a SS-LWA, one might determine C by evaluating the attenuation constant at broadside $\hat{\alpha}_0$ when $r=1$, and thus $C=\hat{\alpha}_0^2$. For such a structure the leakage rate $\hat{\alpha}_0$ of the $\rm TE_2$ mode (the mode responsible for the narrow beam in the H-plane) can be calculated through [14, Eq. (17c)], and is thus equal to $\hat{\alpha}_0=0.14$, leading to $C=\hat{\alpha}_0^2=0.0196$. However, by varying either the substrate thickness or the operating frequency, the value of r changes, but C remains constant as the PRS is not changing. At this point, we wish to find the value of r that minimizes the beamwidth of such a PRS. Using the beamwidth formula, i.e., Eq. (27), we find that the optimum value of r is $r=0.58$, yielding a HPBW of 17.92°. The corresponding value of a is 3.44, corresponding to a radiation efficiency of 99.9%. Using the exact pattern, i.e, Eq. (2), we find that the optimum value of r is $r=0.66$, and the corresponding beamwidth is 18.23° (see Fig. 9). With the optimum value of r now known, one can design the structure at a given frequency by changing the substrate thickness to find the thickness that results in this value of r. Note that because of the very high efficiency obtained in this optimum design, the optimum value of r, which minimizes the beamwidth and thus maximizes the directivity, also maximizes the gain of the LWA.

The second example is one of a metal strip grating leaky-wave antenna (MSG-LWA) [15] with strip width $w=\lambda/25$ and grating period $\lambda/10$. The perfectly conducting strips are printed over a grounded dielectric slab ($\varepsilon_{\rm r}=2.1$ and $h=\lambda/(2\sqrt{\varepsilon_{\rm r}})$ as for the substrate of the first example) of length $L=10\lambda$. For this kind of periodic surface, homogenization formulas can be used to characterize the electromagnetic properties of this PRS with a sheet reactance that is given by [16, Eq. (4.58)] (assuming the electric field polarization is parallel to the strips). For the case considered here, the use of Eq. (4.58) in [16] furnishes an inductive reactance of about $20\ \Omega$. Using this value in [8, Eq. (21)], one can find the value of the leakage rate at broadside $\hat{\alpha}_0=0.0522$, and thus the constant $C=0.0027$ characterizing this PRS. Proceeding as for the SS-LWA, we

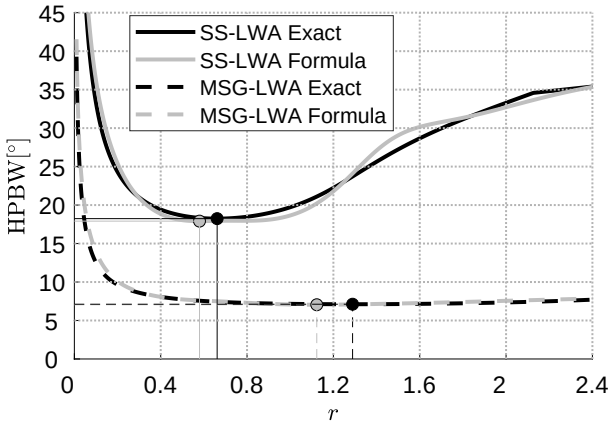

Fig. 9. HPBW vs. r for two different PRS types of LWA structures (parameters in the text): a substrate-superstrate leaky-wave antenna (solid lines) and a metal strip grating LWA (dashed lines). A comparison is shown between the approximate formula (in gray) and the exact pattern (in black). The minimum of each curve is emphasized with a small circle, and the corresponding minimum beamwidths are indicated with horizontal dashed lines.

find that, using beamwidth formula, the optimum value of r is $r = 1.12$, yielding a HPBW of $7.05°$. The corresponding value of a is 1.54, corresponding to a radiation efficiency of 95.5%. Using the exact pattern, i.e, Eq. (2), we find that the optimum value of r is $r = 1.29$, and the corresponding beamwidth is $7.12°$ (see Fig. 9). The corresponding value of a is 1.44, corresponding to a radiation efficiency of 94.4%. The design of the structure then follows as for the SS-LWA. In this second design example the optimum r value will maximize the directivity, but not the gain. The gain could be maximized by approximating the gain as being proportional to the efficiency divided by the beamwidth, and searching for the r value that maximizes this quantity. Details are omitted.

In both the first and the second design examples, the error incurred in the estimation of the optimum r-values by using the beamwidth formula are both about 10%, but the error between the exact and approximate beamwidths are both only about 1%. We notice that in both cases the error between the r-values is much greater than the error between the beamwidths. In this regard, it should be noted that a plot of the beamwidth vs. r is locally flat near the minimum point (see Fig. 9), and this feature tends to magnify the error in the optimum r value that is found by any approximate method that has error in it. By the same token, the change in the beamwidth due to a change in the r value is small, since we are at a minimum.

As a final comment, we briefly discuss also the beamwidth properties of a finite-length 1-D bidirectional LWA radiating in the third-regime. As we have seen in the Subsection III-D, when $r > r_{\rm d}(a)$, a finite-length 1-D bidirectional LWA exhibits a dual beam pointing off-broadside. In general, the pointing angle $\theta_{\rm p}$ of a finite-length 1-D bidirectional LWA is not known in analytical form. However, when $r \gg r_{\rm d}(a)$, the pointing angle can be calculated through Eq. (10). Thus the beamwidth properties of finite 1-D bidirectional LWAs with $\beta \gg \alpha$ are given with good accuracy by the formula for a finite 1-D unidirectional LWA of length L as presented in [5], which we report here for convenience:

$$\Delta\theta_{\rm h} = \theta_{\rm p} - \arcsin\left\{\frac{\beta}{k_0} - \frac{2.783}{k_0 L}\left[1 - \tanh\left(0.021\frac{\alpha L}{2}\right)\right] - \frac{\alpha}{k_0}\tanh\left(0.21\frac{\alpha L}{2}\right)\right\}. \quad (28)$$

In conclusion, Eqs. (27)-(28) now provide a reliable tool for the accurate estimation of the half-power beamwidth of finite-length 1-D bidirectional LWAs, operating in any radiating regime of practical interest.

VI. Conclusion

The beam properties of 1-D bidirectional LWAs have been analyzed in detail. First, it has been shown that, in the infinite-aperture case, it is possible to distinguish three different radiating regimes: in the first one, upper-bounded by the splitting-point condition, the antenna radiates a smooth broadside beam; in the second one, lower-bounded by the splitting-point condition and upper-bounded by the dual-beam condition, the antenna exhibites a scalloped broadside beam; in the third one, lower-bounded by the dual-beam condition, the antenna radiates two symmetric beams pointing off-broadside. In the infinite-aperture case, analytic formulas have been provided for evaluating the beamwidth in any radiating regime, and the results are summarized in Table I.

In the finite-aperture case, it has been shown that the boundaries dictating the splitting-point and the dual-beam conditions are no longer constants, but considerably change as the radiation efficiency changes. Analytical formulas have been provided for correctly predicting the expected radiating regime for any practical design and the results are summarized in Eqs. (19) and (20).

The relevant case of a finite-length 1-D bidirectional LWA radiating in the first and second regimes has been extensively analyzed for different sets of parameters. An exact beamwidth equation has been derived and its numerical evaluation has been performed to derive approximate analytical formulas. A new analytical formula has been provided for accurately evaluating the beamwidth in almost any case of practical interest, and the result is summarized in Eq. (27) together with Eq. (26).

Comparison with previous formulas existing in the available literature has then been made to corroborate the need for these new formulas. The improved accuracy achieved with these new formulas will allow for the simple design of practical 1-D bidirectional LWAs. Due to the strong connection between the radiating properties of 1-D bidirectional LWAs and 2-D LWAs, these results are expected to be pivotal for the characterization of the beamwidth properties of finite 2-D LWAs as well.

References

[1] A. A. Oliner and D. R. Jackson, "Leaky-Wave Antennas," in *Antenna Engineering Handbook*, J. L. Volakis, Ed. New York, NY, USA: McGraw-Hill, 2007, ch. 11.

[2] D. R. Jackson, C. Caloz, and T. Itoh, "Leaky-Wave Antennas," in *Frontiers in Antennas: Next Generation Design & Engineering*, F. Gross, Ed. New York, NY, USA: McGraw-Hill, 2011, ch. 9.

[3] A. Galli, P. Baccarelli, and P. Burghignoli, "Leaky-Wave Antennas," in *The Wiley Encyclopedia of Electrical and Electronics Engineering*, J. Webster, Ed. New York, NY, USA: John Wiley & Sons, 2016.

[4] C. H. Walter, *Traveling Wave Antennas*. Los Altos, CA, USA: Dover Publications, 1970.
[5] W. Fuscaldo, D. R. Jackson, and A. Galli, "A general and accurate formula for the beamwidth of 1-D leaky-wave antennas," *IEEE Trans. Antennas Propag.*, vol. 65, no. 4, pp. 1670–1679, Apr. 2017.
[6] ——, "Beamwidth properties of endfire 1-D leaky-wave antennas," *IEEE Trans. Antennas Propag.*, vol. 65, no. 11, pp. 6120–6125, Nov. 2017.
[7] E. M. O'Connor, D. R. Jackson, and S. A. Long, "Extension of the Hansen-Woodyard condition for endfire leaky-wave antennas," *IEEE Antennas Wireless Propag. Lett.*, vol. 9, pp. 1201–1204, 2010.
[8] G. Lovat, P. Burghignoli, and D. R. Jackson, "Fundamental properties and optimization of broadside radiation from uniform leaky-wave antennas," *IEEE Trans. Antennas Propag.*, vol. 54, no. 5, pp. 1442–1452, May 2006.
[9] P. Burghignoli, G. Lovat, and D. R. Jackson, "Analysis and optimization of leaky-wave radiation at broadside from a class of 1-D periodic structures," *IEEE Trans. Antennas Propag.*, vol. 54, no. 9, pp. 2593–2604, Sep. 2006.
[10] A. Sutinjo, M. Okoniewski, and R. H. Johnston, "Beam-splitting condition in a broadside symmetric leaky-wave antenna of finite length," *IEEE Antennas Wireless Propag. Lett.*, vol. 7, pp. 609–612, 2008.
[11] T. Tamir and A. A. Oliner, "Guided complex waves. Part 1: fields at an interface," *Proc. IEE*, vol. 110, no. 2, pp. 310–324, Feb. 1963.
[12] ——, "Guided complex waves. Part 2: relation to radiation patterns," *Proc. IEE*, vol. 110, no. 2, pp. 325–334, Feb. 1963.
[13] C. A. Balanis, *Antenna Theory: Analysis and Design*. Hoboken, NJ, USA: John Wiley & Sons, 2005.
[14] D. R. Jackson and A. A. Oliner, "A leaky-wave analysis of the high-gain printed antenna configuration," *IEEE Trans. Antennas Propag.*, vol. 36, no. 7, pp. 905–910, Jul. 1988.
[15] P. Burghignoli, G. Lovat, F. Capolino, D. R. Jackson, and D. R. Wilton, "Highly polarized, directive radiation from a Fabry-Perot cavity leaky-wave antenna based on a metal strip grating," *IEEE Trans. Antennas Propag.*, vol. 58, no. 12, pp. 3873–3883, Dec. 2010.
[16] S. Tretyakov, *Analytical Modeling in Applied Electromagnetics*. Norwood, MA, USA: Artech House, 2003.

Walter Fuscaldo (S'15–M'18) received the B.Sc. and M.Sc. (cum laude) degrees in Telecommunications Engineering from Sapienza University of Rome, Rome, in 2010 and 2013. In 2017, he received the Ph.D. degree (cum laude and with the *Doctor Europaeus* label) from both the Department of Information Engineering, Electronics and Telecommunications (DIET) and the Institut d'Électronique et de Télécommunications de Rennes (IETR), Université de Rennes 1, Rennes, France, under a cotutelle agreement between the institutions.

In 2014, 2017, and 2018, he was a Visiting Researcher with the NATO-STO Center for Maritime Research and Experimentation, La Spezia, Italy. In 2016, he was a Visiting Researcher with the University of Houston, Houston, TX, USA. His current research interests include propagation of leaky waves, surface waves and surface plasmon polaritons, analysis and design of leaky-wave antennas, generation of limited-diffraction limited-dispersion electromagnetic waves, millimeter-wave focusing systems, graphene electromagnetics, metasurfaces, and THz antennas.

Dr. Fuscaldo was a recipient of the Yarman-Carlin Student Award at the IEEE 15th Mediterranean Microwave Symposium in 2015, and he was awarded the Young Engineer Prize for the Best Paper presented at the 46th European Microwave Conference in 2016, the IEEE AP-S Student Award, Chapter Center-Southern Italy in 2017, the Best Paper in Electromagnetics and Antenna Theory at the 12th European Conference on Antennas and Propagation in 2018, the "Barzilai Prize for the best scientific work of under-35 researchers at the "22th National Meeting of Electromagnetics, and the Publons Peer Review Award 2018 for placing in the top 1% reviewers in Engineering on Publons global reviewers database, determined by the number of peer review performed during the 2017–2018 Award year.

David R. Jackson (F'99) David R. Jackson was born in St. Louis, MO on March 28, 1957. He obtained the B.S.E.E. and M.S.E.E. degrees from the University of Missouri, Columbia, in 1979 and 1981, respectively, and the Ph.D. degree in electrical engineering from the University of California, Los Angeles, in 1985. From 1985 to 1991 he was an Assistant Professor in the Department of Electrical and Computer Engineering at the University of Houston, Houston, TX. From 1991 to 1998 he was an Associate Professor in the same department, and since 1998 he has been a Professor in this department. He has been a Fellow of the IEEE since 1999. His present research interests include microstrip antennas and circuits, leaky-wave antennas, leakage and radiation effects in microwave integrated circuits, periodic structures, and electromagnetic compatibility and interference. He is presently serving as the Immediate Past Chair of USNC-URSI, the U.S. National Committee (USNC) for URSI, the International Union of Radio Science. From 2015-2018 he served as the Chair of USNC-URSI. He is also on the Education Committee of the Antennas and Propagation Society (AP-S) and on the MTT-15 (Microwave Field Theory) Technical Committee of the Microwave Theory and Techniques Society.

Previously, he has been chair of the Distinguished Lecturer Committee of the IEEE Antennas and Propagation Society (AP-S), the chair of the Transnational Committee of the IEEE AP-S, the chair of the Chapter Activities Committee of the AP-S, a Distinguished Lecturer for the AP-S, a member of the AdCom for the AP-S, and an Associate Editor for the IEEE Transactions on Antennas and Propagation. He previously served as the chair of the MTT-15 (Microwave Field Theory) Technical Committee. He has also served as the chair of Commission B of USNC-URSI and as the Secretary of this Commission. He also previously served as an Associate Editor for the Journal Radio Science and the International Journal of RF and Microwave Computer-Aided Engineering.

Alessandro Galli (S'91-M'96) received the Laurea degree in Electronic Engineering and the Ph.D. degree in Applied Electromagnetics from Sapienza University of Rome, Rome, Italy. Since 1990, he has been with the Department of Electronic Engineering (now Department of Information Engineering, Electronics and Telecommunications, DIET), Sapienza University of Rome. In 2000, he became an Assistant Professor, and in 2002 an Associate Professor at the Faculty of Engineering, Sapienza University of Rome. In 2013, he won the National Scientific Qualification as a Full Professor in the sector of Electromagnetics. Dr. Galli has authored more than 300 papers on journals, books, and conferences. He is author of a patent for an invention concerning a type of microwave antenna. His research interests include theoretical and applied electromagnetics, mainly focused on modeling, numerical analysis, and design for antennas and passive devices at microwaves, millimeter waves, and terahertz: specific topics involve leaky waves, periodic and multilayered printed structures, metamaterials, and graphene. He is active also in geoelectromagnetics, bioelectromagnetics, and microwave plasma heating for alternative energy sources. In 2014, he was the general co-chair of the "European Microwave Week" (EuMW), the most important conference event in the electromagnetic area at European level. He was elected as the Italian representative of the Board of Directors of the "European Microwave Association" (EuMA), the main European Society of electromagnetics, for the 2010-2012 triennium and then re-elected for the 2013-2015 triennium. Since its foundation in 2013, he is the coordinator of the "European Courses on Microwaves" (EuCoM), the first European educational institution on microwaves. He is also a member of the "European School of Antennas" (ESoA). He is a member of the leading scientific societies of electromagnetics, and an Associate Editor of the "International Journal of Microwave and Wireless Technologies" (by Cambridge University Press) and of the "IET Microwaves, Antennas & Propagation" (by the Institution of Engineering and Technology). He was the recipient of various grants and prizes for his research activity: he won in 1994 the "Barzilai Prize" for the best scientific work of under-35 researchers at the "10th National Meeting of Electromagnetics" and, in 1994 and in 1995, the "Quality Presentation Recognition Award" at the International Microwave Symposium by the "Microwave Theory and Techniques" (MTT) Society of the "Institute of Electrical and Electronics Engineering" (IEEE).